Hydrogen Production through Polyoxometalate Catalysed Electrolysis from Biomass Components and Food Waste

Results in Engineering 23 (2024) 102803

Contents lists available at ScienceDirect

Results in Engineering

journal homepage: www.sciencedirect.com/journal/results-in-engineering

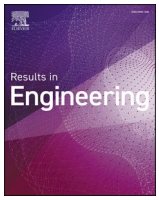

Hydrogen production through polyoxometalate catalysed electrolysis from biomass components and food waste

Muhammad Umer [a,*], Caterina Brandoni [a], Svetlana Tretsiakova [a], Neil Hewitt [a], Patrick Dunlop [b], M.D. Mokim [a], Kai Zhang [c], Ye Huang [a]

[a] Centre for Sustainable Technologies, School of Architecture and the Built Environment, Ulster University, Belfast, BT15 1ED, UK
[b] NIBEC, School of Engineering, Ulster University, Belfas, BT15 1ED, UK
[c] School of Energy Power and Mechanical Engineering, North China Electric Power University, Beijing, 102206, PR China

ARTICLE INFO

Keywords:
Electrolysis
Biomass
Food waste
Hydrogen production
Polyoxometalate catalyst

ABSTRACT

Electrolysis from biomass is a promising process for hydrogen generation from biomass and biowaste that is still unexplored. The paper used lignocellulosic biomass components and food waste (banana and cucumber peels) as feedstocks to explore hydrogen generation through an H-type proton exchange membrane electrolytic cell. Polyoxometalates (PMo_{12}) were employed as a catalyst and charge carrier during the pre-treatment stage in the biomass degradation process. Electrochemical characterisations were conducted in a potential range of 0–1.20 V to analyse the electrochemical reaction behaviour at the anode. To assess the impact of temperature on the hydrogen yield rates, the electrolysis was conducted at both room temperature (19 °C) and a higher temperature (80 °C). Results show that the maximum hydrogen produced in the first hour was 7.8 mL per gram of biomass. With an electrical potential of 1.20 V and a temperature of 80 °C, the hydrogen yield rate of glucose was three times higher than that of the individual biomass components, i.e., cellulose, lignin, hemicellulose, and starch. The volume of hydrogen yielded from banana peel and cucumber was 49.2 mL and 39.6 mL, respectively. The overall conversion efficiency was calculated as the weight percentage ratio of the hydrogen contained in cucumber and banana peels and the hydrogen collected was 10 % and 17 %, respectively, suggesting the need to identify solutions to extract the hydrogen content from biomass material further.

1. Introduction

Reducing greenhouse gas emissions is one of the most pressing issues in today's world, triggering demands for sustainable energy from carbon-neutral and renewable resources [1,2]. To overcome the persisting challenge of global warming, there is a growing interest in the generation of hydrogen (H_2) as an alternative to the dwindling fossil fuels [3,4]. Hydrogen is considered a clean energy source because it produces no emissions when used as a fuel. Furthermore, it has the highest heating value among all hydrocarbons, i.e., 141.8 MJ/kg [5]. Currently, the primary methods for H_2 generation on a commercial scale are water electrolysis and steam reforming of natural gas [6–8]. Nevertheless, the current technologies are still challenged by high-grade energy consumption (i.e. water electrolysis), the non-renewability of the sources (steam reforming) and abundant energy losses [9]. Biomass is an additional renewable source that can produce hydrogen [8] and has recently gained attention [10,11]. Various technologies have been used to generate hydrogen from biomass, including thermo-chemical conversion, biochemical processes, photo-electrochemical methods, and electrolysis [12,13]. Among these, thermo-chemical techniques like pyrolysis and gasification show potential for large-scale hydrogen production by utilising forestry and agricultural residues [14]. However, these methods face significant challenges, such as catalyst durability, thermal efficiency, and product impurities [15]. Similarly, the biochemical conversion processes such as fermentation and anaerobic digestion are selective regarding feedstocks, requiring starch and sugar-rich feedstocks, and face challenges in directly processing lignocellulosic materials [16]. A critical issue for hydrogen generation through the technologies mentioned above is the purity of the H_2 collected. For example, in the gasification, pyrolysis, and anaerobic fermentation processes, the end products are a mixture of gases such as CO, CO_2, H_2 and methane, which increases the cost of the process to separate H_2 from other gases [17]. Photocatalytic hydrogen production from biomass is an emerging technology offering innovative hydrogen

* Corresponding author.
E-mail address: umer-m2@ulster.ac.uk (M. Umer).

https://doi.org/10.1016/j.rineng.2024.102803
Received 18 June 2024; Received in revised form 10 August 2024; Accepted 28 August 2024
Available online 30 August 2024

synthesis pathways. Still, it is limited by low yield and the need for noble metal catalysts [18].

Electrolysis from biomass is a promising technology which can work at relatively low temperatures [19]. It has several advantages, including (i) high H_2 purity, (ii) reaction velocity, (iii) lower energy requirement compared to water electrolysis, (iv) the possibility to work with high moisture biomass and (v) low carbon footprints [20].

Although biomass electrolysis has many benefits, there are still challenges to its commercial implementation. These include the need to (i) improve the hydrogen conversion efficiency [21], (ii) determine the best way to extract more carbon from the electrolysis residue (which is still high, especially when using pure biomass) [22], and (iii) optimise the biomass degradation [19,23]. For this, there is a pressing need to identify advanced materials or catalysts that can degrade biomass, being electrochemically stable and reusable or recoverable from the biomass solution. Recent studies have focused on $CeVO_4$/rGO [24,25], SmRE-Ti_2O_7 pyrochlores [26], $Nd_2Sn_2O_7$ nanostructures [25] and $Dy_2Ce_2O_7$ nanostructures [27]. Developing such catalysts could significantly enhance the efficiency and sustainability of the hydrogen production process, ensuring it is both economically viable and eco-friendly.

Two technologies can be applied for biomass electrolysis: (i) microbial electrolysis cell (MEC) [28] and (ii) proton exchange membrane (PEM) electrolysis cell [29]. However, significant concerns exist with MEC technology, such as (i) lignocellulosic biomass cannot be directly utilised as feedstock for H_2 formation, and it must first be fermented to low-molecular-weight compounds or monosaccharide [30], (ii) slower fermentation speed due to limited lifetime or stability of microorganisms leads to slow H_2 rate, (iii) low process efficiency [19] and (iv) product purity (contain mixture of H_2, CO_2 and other gases) [31]. PEM electrolysis cell, on the other hand, does not require fermentation and is easy to operate; it employs a proton exchange membrane (PEM), which provides H_2 purity and facilitates the transitions of protons (H^+) via the membrane to the cathode, increasing the H_2 production rate [32–34].

Recent experimental studies have explored biomass electrolysis for hydrogen production from various feedstocks using PEM electrolysis cells. For example, hydrogen was produced from cornstalk degraded by $FeCl_3$ solution via proton exchange membrane (PEM) electrolysis, achieving a yield of 2 mL with a Faraday efficiency of 94.65 % at a current density of 5 mA cm^{-2} [35]. Another study depicts that an aqueous solution of lignin and 1M NaOH was used in a PEM electrolysis cell at 80–90 °C to generate hydrogen, achieving a rate of 0.4 μmol s^{-1} with a current density of 3.6 mA cm^{-2} [36]. Additionally, waste newspaper treated with 85 % H_3PO_4 under a temperature range of 125–175 °C was processed in a flow PEM cell at 150 °C, producing 0.2 g of hydrogen per gram of newspaper across a current density range of 0.15–0.25 A cm^{-2} [37]. Miscanthus synesis was also used as energy grass in a flow PEM cell operated at 150 °C, achieving a maximum current density of 0.254 A cm^{-2} for electrolysis [38]. These studies revealed that biomass electrolysis could be achieved at lower electrical voltage starting from 0.1 V compared to water electrolysis [19,39]. Despite these advances, most of these studies involved extreme conditions such as high temperatures and toxic chemicals as oxidising agents for the degradation of biomass materials, which diminished the overall process energy efficiency and environmental sustainability. Therefore, to achieve efficient H_2 generation through raw biomass, a highly active catalyst or oxidising agent is required to degrade and catalyse the polymeric biomass at low-temperature conditions.

Polyoxometalate (PMo_{12}) has recently gained interest from researchers due to its significant potential as a catalyst or redox mediator, its possibility of working at low temperatures and its reusability [17]. PMo_{12} is a transition metal-oxygen cluster with diverse physical and chemical properties, including high charge storage capacity, great potential for oxidation degradation and multi-electron reduction ability [40,41]. Numerous studies have been reported for H_2 generation using PMo_{12} via the electrolysis process. Li et al. [42] recently used PMo_{12} to convert corn straw to H_2 energy through an h-type PEMEC electrolysis process at 80 °C. The reported amount of H_2 was 7.86 mL/h at a constant current density of 20 mA cm^{-2}. In another study, Ting wang et al. [20] used PMo_{12} to determine the volume of H_2 through lignin in h-type PEMEC. The maximum reported volume of H_2 was 7.92 mL/h at 20 mA cm^{-2} constant current density. Price et al. [43] employed a two-stage electrolysis process to convert liquid whiskey co-products into hydrogen using a PMo_{12} catalyst, resulting in 26 cm^3 of H_2 formation via a PEM flow cell at a current density of 50 mA cm^{-2}. Similarly, Deng et al. [44] used PMo_{12} as a charge carrier/catalyst for directly converting biomass to electricity through fuel cells. The maximum power density reached 0.72 mW cm^{-2} via cellulose, which was 100 times higher than a microbial fuel cell. The mechanism study of the biomass electrolysis system reveals that PMo_{12} and biomass feedstock undergo an oxidation-reduction reaction during the thermal digestion process. PMo_{12} becomes reduced (H-$PMo_{12\ reduced}$) during the catalytic redox reaction with biomass upon heating, and the biomass is oxidised and degraded [43]. The H-$PMo_{12\ reduced}$ reoxidised (H- $PMo_{12\ oxidised}$) to its original form at the anode by applying electric potential and releasing electrons (e^-) and H^+ simultaneously during electrolysis [45]. These generated protons (H^+) travel across the PEM membrane and spread at the cathode to synthesise H_2 [20]. Therefore, the oxygen evolution reaction (OER) at the anode typically seen in water electrolysis is replaced with the oxidation reaction of H-$PMo_{12\ reduced}$ during biomass electrolysis. The hydrogen gas produced derives from the hydrogen content of the biomass feedstocks rather than from water molecules [35].

The present paper aims to understand the correlation between the hydrogen production of main biomass components (i.e. glucose, starch, lignin, cellulose, hemicellulose) and biomass, which has yet to be thoroughly discussed by the current literature. The influence of the main operating parameters, pre-treatment duration and temperature, electrolysis operating temperature and the time variation of hydrogen generation are presented and discussed. Furthermore, the study demonstrates the feasibility of generating hydrogen from food waste via electrolysis. Currently, one-third of the food produced in the world is wasted. According to the WARP 2023 report, the UK produces approximately 9.5 million tonnes of food waste annually, emitting around 25 million tonnes of greenhouse gases, including CO_2 and methane (CH_4) [39]. To the authors' knowledge, this is the first time food waste (banana and cucumber peel) has been tested for biomass electrolysis; researchers have focused so far on traditional biomass feedstocks, such as corn straw [46], wood waste [17], and energy crops [47].

2. Materials and methods

2.1. Materials

Phosphomolybdic acid ($H_3PMo_{12}O_{40}$, also known as PMo_{12}, in its anhydrous form) and phosphoric acid (H_3PO_4, with a concentration of 85 %), both purchased from Alfa Aesar, UK, Nafion 117 (DuPont), a proton exchange membrane (PEM) with a thickness of 183 μm, was purchased from Ali express. Sulfuric acid (H_2SO_4, 95–98 %) and hydrogen peroxide (H_2O_2, 30 %) were procured from Alfa Aesar, UK. The biomass components, including microcrystalline cellulose ($(C_6H_{10}O_5)_n$, average particle size: 50 μm), starch ($(C_6H_{10}O_5)_n$, from potato), and glucose ($C_6H_{12}O_6$, 99 %), were purchased from Alfa Aesar, UK. Additionally, lignin (alkali) was purchased from Sigma-Aldrich, UK, and hemicellulose (xylan) from Apollo-Scientific, UK. The chemicals used in this research study were not subjected to any further purification. The two raw biomasses, banana peel and cucumber peel were obtained from kitchen waste. They were dried and ground into powder form without undergoing chemical purification for experimental investigations.

2.1.1. Selection of feedstocks

Glucose, starch, lignin, hemicellulose, and cellulose were selected due to their significant presence in biomasses and abundance in organic

materials. For example, wheat straw contains 34.4 wt % cellulose, 23.6 wt % lignin, and 19.5 wt % hemicellulose [48]; rice straw is composed of 47 wt % cellulose, 24 wt % lignin, and 37 wt % hemicellulose [49]; and wheat meal contains 72.2 wt % starch [50]. Table S1 details the elemental analysis of the selected feedstocks for the experimental study.

In addition to the biomass components, banana and cucumber peels were chosen. The primary criteria for selecting banana and cucumber peels, among other food wastes, is that they are two of the top five food waste streams in the UK. Secondly, they were selected for the presence of hydrogen in their elemental composition and their lignocellulosic composition. Table S2 shows the lignocellulosic content of both banana and cucumber peels.

2.2. Experimental

2.2.1. Pre-treatment stage

The biomass electrolysis process relies on chemical pre-treatment, essential for degrading biomass feedstock. Due to their complex structural configuration, this step is necessary for solubilising and hydrolysing biomass materials [20]. In this research, we pretreated pure biomass components such as cellulose, lignin, starch, hemicellulose and glucose, as well as raw biomasses (dry) like banana peel and cucumber peel before electrolysis, to break down their complex and rigid polymeric structure. A reflux pre-treatment system consisting of a hot plate, condenser, pipes, and round glass flask was designed. In this process, 0.5 g (g) of biomass was mixed with a 0.1 M PMo_{12} solution in the flask, and the solution's total volume was adjusted to 50 mL. After that, the mixed solution of biomass-PMo_{12} was heated in an oil bath at 100 °C for 4 h, as illustrated in Fig. S1 (a). The prepared biomass-PMo_{12} electrolyte solution was then subjected to an electrochemical study.

2.2.2. Biomass electrolysis stage

The experiments were conducted using a 50 mL H-type Proton Exchange Membrane Electrolysis Cell (PEMEC), a batch process system, as depicted in Fig. S1 (b). The H-PEMEC system comprises two glass chambers, known as the anode and cathode chambers, separated by a Nafion 117 proton exchange membrane (PEM) and connected by a steel clutch. For the electrochemical reactions two electrodes were used: a 6 mm graphite anode (positive electrode) and a 1 cm^2 platinum mesh cathode. Before utilised Nafion 117 PEM was thoroughly purified and cleaned in 1 M sulfuric acid (H_2SO_4) and 3 % hydrogen peroxide (H_2O_2) and boiled for 1 h at 100 °C. It was then rinsed and soaked in distilled water for 20 min before being used in the H-PEMEC. The electrolysis tests were performed by applying an electric potential of 1.20 V using a PalmSens4 Potentiostat at 80 °C and ambient temperature (19 °C). However, a thermal oil bath served as the heat source for the electrolysis cell and a water displacement system was utilised to collect hydrogen from the cathode unit.

The conditions set to perform biomass electrolysis experiments were an anolyte consisting of a pretreated solution of 0.1 mol L^{-1} PMo_{12} and 0.5 g of the biomass components and dry banana and cucumber peels, pretreated for 4 h at 100 °C; a catholyte of 1 mol L^{-1} H_3PO_4 solution; the use of a graphite rod as the anode and a platinum mesh as the cathode; a solution volume of 50 mL for both anode and cathode sides. Blank tests were conducted under the same experimental conditions to verify hydrogen evolution without biomass feedstock and PMo_{12}. In all the experiments, the concentration of PMo_{12} was maintained at 0.1 mol L^{-1}. This specific concentration was selected as optimal based on the existing literature [42]. Moreover, various electrochemical characterisation techniques such as cyclic voltammetry (CV), linear sweep voltammetry (LSV), electrochemical impedance spectroscopy (EIS), and chronoamperometry (CA) were employed to analyse the reaction kinetics of the PMo_{12}-mediated biomass solutions during electrolysis using a PalmSens4 Potentiostat. To identify the structural bonding of banana and cucumber peels and the reduction of PMo_{12}, Fourier transform infrared spectrometer (Thermo Nicolet, Nexus spectrometer) and UV–visible (Evolution 220 UV–visible spectrophotometer) characterisations were employed.

3. Results and discussions

3.1. Electrochemical investigation of biomass components via PMo_{12}

Multiple experiments were performed to assess the electrochemical performance (i.e., current vs voltage (I vs V) relationship) of biomass component-PMo_{12} mixtures, including glucose-PMo_{12}, starch-PMo_{12}, lignin-PMo_{12}, hemicellulose-PMo_{12}, and cellulose-PMo_{12} as shown in Fig. 1(a and b). These electrochemical tests were conducted within a potential range of 0–1.20 V, at a scan rate of 0.5 mV/s, and 80 °C, considered the baseline electrolysis operating temperature. Fig. 1a shows the (I vs V) curves of biomass electrolysis. No significant current was detected when the control electrolysis experiment was conducted without biomass feedstocks and PMo_{12} catalyst in the PEMEC electrolysis system, even at an applied electric potential of 1.20 V. The lack of current during the blank test suggests that biomass and PMo_{12} alone cannot produce H_2 without biomass components (i.e., glucose, starch, lignin, hemicellulose and cellulose), within the 0–1.20 V potential range.

Introducing biomass components into the PMo_{12} solution significantly increased the electrolytic current, with observable hydrogen bubbles forming at the cathode during the electrolysis process. The polarisation curves (I vs V) in Fig. 1a illustrate that at the beginning of the reaction, the current densities were low within an applied potential range of 0–0.4 V. As the applied voltage crossed 0.5 V, there was a slight increase in electrolysis current density. The upward trend became more significant when the applied electric potential exceeded 0.6 V, coinciding with the noticeable H_2 gas bubbles formation at the cathode unit.

Fig. 1 reveals that the onset potential (the value at which the density current increases) varies among the biomass components. As discussed in the literature, the variation is likely attributed to the biomass feedstocks' complex polymeric structure, which impacts the reduction degree of PMo_{12} [17].

The reduction degree of PMo_{12} is described by the average number of electrons transferred from biomass to 1 mol of the PMo_{12} anion during the thermal digestion of biomass [51]. Upon heating or pre-treatment, a redox reaction occurs. This interaction leads to the oxidation or degradation of the biomass while PMo_{12} is reduced [52]. In this redox reaction, biomass acts as an electron donor, while PMo_{12} acts as an electron acceptor. The electrons transferred from the biomass reduce PMo_{12}, which is re-oxidised at the anode during electrolysis, releasing electrons and protons that facilitate hydrogen production at the cathode. The degree of reduction of PMo_{12} indicates its efficiency in accepting electrons. Increased acceptance of electrons by PMo_{12} during the redox reaction enhances the degradation of biomass and as a result, more H-$PMo_{12\ reduced}$ is available during the electrochemical reaction [20]. This higher availability of H-$PMo_{12\ reduced}$ facilitates a higher electrolytic current, boosting hydrogen production [53].

The onset potentials for glucose and starch were approximately 0.55 V, whereas lignin, hemicellulose and cellulose exhibited higher onset potentials in the 0.7–0.8 V range. The lower onset potentials for glucose and starch can be explained by their ease of degradation and hydrolysis by PMo_{12}, which aligns with the literature [54]. Due to their complex and rigid crystalline structures, lignin, hemicellulose, and cellulose show slightly higher onset potentials [44].

We chose a 1-h experiment time to compare the hydrogen production of different feedstocks. For glucose, a maximum current density of 19.03 mA cm^{-2} was recorded, and the hydrogen generation reached 7.8 mL at an electric potential of 1.20 V. In comparison, starch, lignin, hemicellulose, and cellulose yielded current densities of 16.27 mA cm^{-2}, 14.78 mA cm^2, 13.76 mA cm^{-2} and 8.11 mA cm^{-2}, respectively, which were approximately 1–3 times lower than that of glucose. The hydrogen production rates after 1 h of electrolysis from starch, lignin,

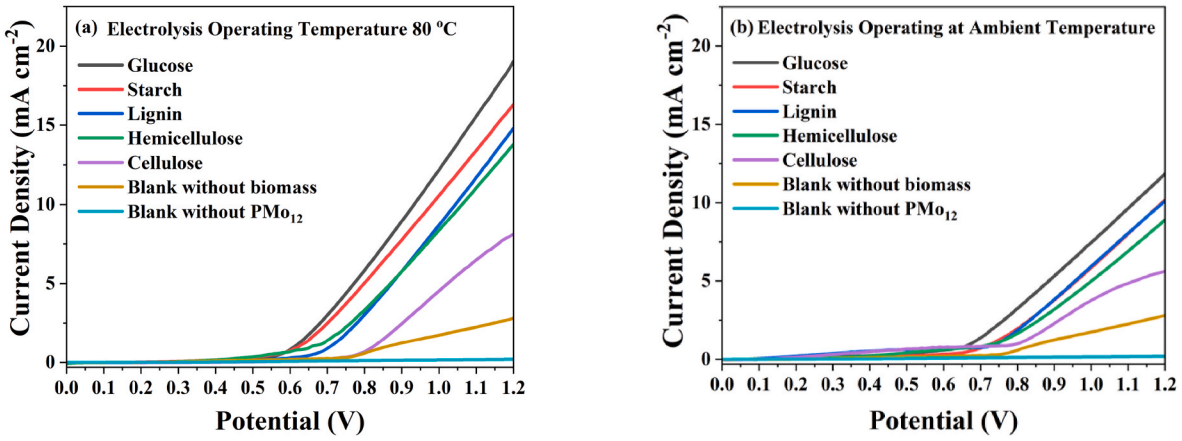

Fig. 1. Polarisation curves (I vs V) of different components of biomass at (a) 80 °C electrolysis temperature and (b) ambient (19 °C) electrolysis operating temperature.

hemicellulose, and cellulose were 6.6 mL, 6.2 mL, 5.9 mL, and 2.6 mL, respectively, 1 to 3 times lower than those obtained from glucose. The higher current density and H_2 yield with glucose compared to other biomass components is still attributed to its ease of decomposition compared to other biomass components [55]. Glucose, a class of sugar, possesses high solubility in water, as shown in Table 1, which facilitates its easy decomposition by PMo_{12} during pre-treatment, releasing a significant number of electrons to PMo_{12} and forming H-$PMo_{12\ reduced}$ [17]. These H- $PMo_{12\ reduced}$ are then electrically oxidised at the anode during the electrolysis process to release electrons and protons simultaneously to generate electrolysis current through the external circuit and H_2 at the cathode [56]. In contrast, as discussed in our previous study [22], starch, lignin, hemicellulose, and cellulose have relatively more complex structures than glucose. Furthermore, according to the elemental analysis, cellulose has higher hydrogen content than lignin and hemicellulose. Therefore, more hydrogen should have been produced. Still, results were in the opposite direction, i.e., lower H_2 yield and electrolysis current were obtained with cellulose, and this finding aligns well with other scientific studies [20,22]. The result indicates that, although a higher hydrogen content in biomass feedstocks might suggest a more significant potential for H_2 generation, structural composition plays a key role.

3.2. Study of electrolysis operating temperature on polarisation curves

To obtain information about the influence of temperature on the electrochemical current (I vs V) during electrolysis, numerous experiments were performed with glucose, starch, lignin, hemicellulose and cellulose using the same experimental conditions at ambient temperature (i.e., 19 °C) and electrolysis operating temperature (80 °C) as shown in Fig. 1(a and b). Fig. 1 b shows that glucose, starch, lignin, hemicellulose and cellulose generated lower electrochemical current when PMo_{12}-mediated-biomass electrolysis operation was conducted at ambient temperature at an electric potential range of 0–1.20 V. The maximum current densities achieved with various biomass components at ambient temperature and 80 °C are shown in Table 2.

Higher current densities were achieved when electrolysis experiments were conducted at 80 °C (i.e., Table 2). The increase in the maximum current density with higher operating temperature depends on a series of factors: (i) enhanced ions mobility [59], i.e., H-$PMo_{12\ reduced}$ is more available to the electrode surface, resulting in increased electrochemical reaction, (ii) lower viscosity: when the temperature rises, the viscosity of the electrolyte solution reduces, improving the electrolyte flow [60], resulting in lower resistance (iii) low polarisation effect; polarisation (i.e. refers to the accumulation of reaction products between the electrode and the electrolyte, which impedes further electrochemical reactions) generally decreases with the rising temperature of the electrolytic solution, enabling electrochemical processes to continue more effectively due to enhanced mobility of reactants and products at the electrode surface [61] and (iv) electrical conductivity: the electrical conductivity of the graphite electrode increases as the temperature rises, due to the higher thermal motion of electrons in graphite atoms, resulting in high electrical conductivity and current density due to lower resistance to the flow of electrical current across the external circuit [22].

3.3. Influence of electrolysis operating temperature on hydrogen generation

To understand the effect of electrolysis operating temperature towards H_2 production, a comparison of all four biomass components towards H_2 yield at ambient (19 °C) and 80 °C is shown in Fig. 2. In line with what is observed for the current densities, the H_2 yield also increases with temperature. The maximum amount of H_2 after 1 h of

Table 1
Molecular size and solubility characteristics of biomass components.

Compound	Molecular Formula	Molecular Size (g/mol)	Solubility Characteristics	References
Glucose	$C_6H_{12}O_6$	~1 nm	Highly soluble in water	–
Lignin	Variable polymeric	10–100 μm	Insoluble in water, varies with solvent	[57]
Cellulose	$(C_6H_{10}O_5)_n$	50 μm	Insoluble in water and most of the solvent	Sigma Aldrich
Hemicellulose	Variable polymeric	~31 μm	Partially soluble in water	[58]

Table 2
Current densities of four biomass components, glucose, starch, lignin and cellulose at an applied voltage range of 0–1.20 V at ambient temperature and 80 °C.

Biomass Components	Electrolysis Operating Temperature (°C)	Maximum Current Density (mA cm^{-2})
Glucose	Ambient (19 °C)	11.84
Glucose	80	19.03
Starch	Ambient	10.17
Starch	80	16.27
Lignin	Ambient	10.10
Lignin	80	14.78
Hemicellulose	Ambient	8.89
Hemicellulose	80	13.76
Cellulose	Ambient	5.62
Cellulose	80	8.11

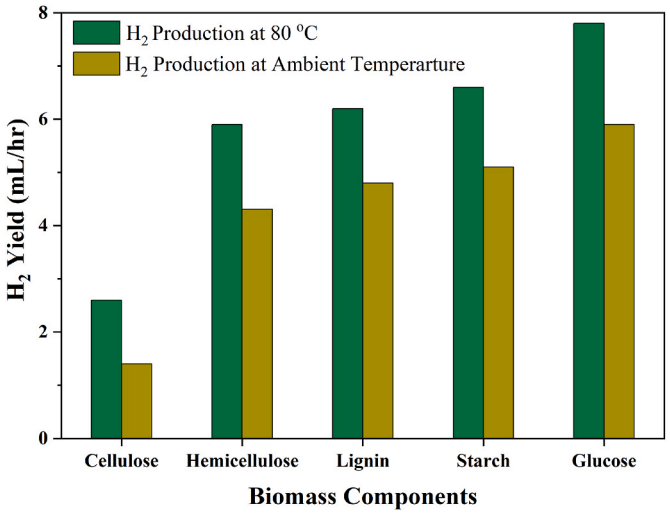

Fig. 2. Hydrogen production rate of different biomass components at a fixed electrolysis time of 1 h.

electrolysis at an applied voltage of 1.20 V was registered for glucose. As discussed above, the increased electric conductivity and reaction rate at higher temperatures translate into higher current density and H_2 production rate [46].

The higher temperature increases the H_2 production, on average, by 25 %. The choice to run the biomass electrolysis at ambient temperature may be based on the reduced energy cost. Table S3 compares the results gathered for H_2 production with the literature, showing the experiments' validity.

3.4. Influence of pre-treatment conditions on hydrogen generation

To investigate the pre-treatment conditions, such as time and temperature on hydrogen production, several experiments were performed with glucose under the following conditions: 0.1 mol L^{-1} PMo_{12}, 0.5 g glucose and a total volume of solution 50 mL. The solution of glucose and PMo_{12} was pretreated at 50 °C, 80 °C and 100 °C for 4 h (baseline pre-treatment time) used in the previous experiments. Fig. S2 (a-b) shows the effect of the pre-treatment temperature on the H_2 yield and current densities during the electrolysis process. The polarisation curves (Fig. S2 (a)) show a maximum current density of 10.01 mA cm^{-2}, 15.47 mA cm^{-2} and 19.03 mA cm^{-2} when glucose was pretreated at 50 °C, 80 °C and 100 °C, respectively. As expected, a similar trend (Fig. S2 (b)) was registered for H_2 production. The H_2 yield in 1 h was 2.8 mL, 6.2 mL, and 7.8 mL at 50 °C, 80 °C, and 100 °C, respectively. The results show that the higher the pre-treatment temperature is, the higher the maximum current density and hydrogen production. There is a linear correlation between the electrolysis current and hydrogen production. The higher pre-treatment time and temperature enable a deeper breakdown of the biomass structure into smaller molecules, enhancing chemical reaction kinetics and promoting solubility of biomass components [62].

The impact of pre-treatment duration on current densities and H_2 yield was also explored using the same PMo_{12}-glucose solution. The investigation was performed over pre-treatment time of 2 h, 4 h and 6 h using the baseline temperature of 100 °C. It can be observed from Fig. S3 that the pre-treatment time can impact the performance of the biomass electrolysis process towards H_2 evolution and electrolytic current. When the solution was pretreated for 2 h, the obtained current density was 17.61 mA cm^{-2} and the H_2 yield was 6.6 mL, which raised to 19.03 mA cm^{-2} and 7.8 mL, respectively, when the pre-treatment was carried out for 4 h. Again, the increase in electrolytic current and H_2 with pre-treatment time is expected to come from the degradation of biomass elemental molecules, which release more electrons and protons, resulting in a higher reduction of PMo_{12}. Furthermore, the solution may contain inhibitory compounds, including polyphenols and organic acids, and inorganic containments, i.e. heavy metals and metal complexes, that can interfere with and limit the electrochemical reactions [17,63]. Therefore, an extended pre-treatment duration helps degrade and remove these inhibitory substances, resulting in better electrochemical performance and higher H_2 yield and electrolytic current. When the pre-treatment duration was prolonged to 6 h, the current and H_2 yield did not increase significantly, suggesting that the degradation may have approached a saturation point, and further extension in the pre-treatment time has no substantial impact on the electrolytic current.

3.5. Electrochemical characterisations and H_2 generation through food waste

Experiments were conducted using banana peel and cucumber peel as raw biomass materials to understand the potential of biomass electrolysis on food waste. These experiments were carried out in an H-type PEMEC. Based on the previous experiments, the parameters set for this study included PMo_{12} concentration of 0.1 mol L^{-1}, biomass concentration of 0.5 g, and pre-treatment of 4 h at 100 °C. The polarisation curves (I vs V) for both the PMo_{12}-banana peel and PMo_{12}-cucumber peel solutions were recorded at an applied potential range of 0–1.2 V, with the scan rate of 0.5 mV/s, as shown in Fig. 3.

The polarisation curves indicate that current density suddenly increases after 0.6 V for both biomass feedstocks and the maximum current density reaches 13.82 mA cm^{-2} and 15.47 mA cm^{-2} for cucumber and banana peel, respectively. The maximum amount of H_2, obtained after 1 h of electrolysis at 1.20 V was 5.9 mL and 6.8 mL for cucumber and banana peels.

Electrochemical impedance spectroscopy (EIS) was performed to understand the reaction kinetics and polarisation resistance within the PEMEC. Fig. S4 (a-b) shows the EIS spectra of the cell with banana peel and cucumber peel, at various applied voltages, including 0.6 V, 0.8 V, 1.0 V, and 1.20 V, across the frequency range of 400 Hz–5 Hz vs. Ag/AgCl. The impedance spectra exhibited distinct features with the increase in voltage. All the curves display a semicircular pattern, suggesting the presence of charge transfer resistance and double-layer capacitance effects [64,65]. When analysing the EIS spectra of both PMo_{12}-banana and PMo_{12}-cucumber peel solutions, a significant change was observed in the charge transfer resistance ($R_{(CT)}$) to the electrode with changing voltage. The grey curve (0.6 V) shows lower resistance, indicating that the reaction is near to start at the graphite electrode

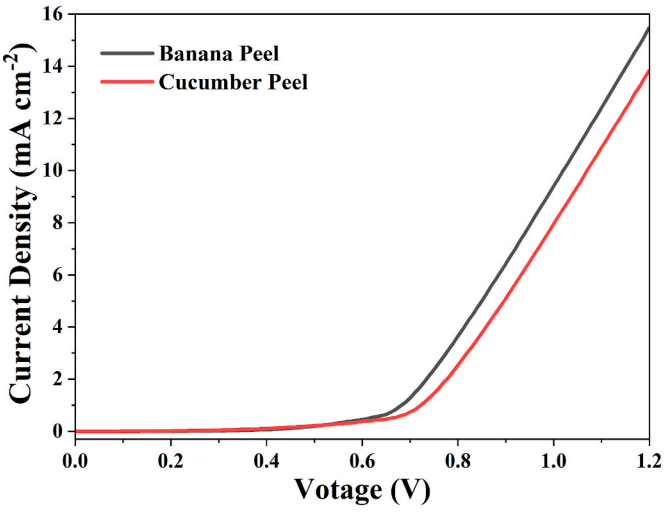

Fig. 3. Linear sweep voltammetry of PMo_{12}-banana and PMo_{12}-cucumber peels at an applied voltage range of 0–1.20 V.

because the redox potential of PMo_{12} is 0.60 V [17]. The red curve (0.8 V) and blue curve (1.0 V) exhibit higher impedance, suggesting higher resistance to charge transfer due to mass transfer limitations and the acceleration of the electrochemical reaction with increasing voltage [38]. This charge transfer resistance decreases when the voltage reaches 1.20 V (green curve), depicting a possible change in the reaction mechanism or improved mass transfer efficiency [66]. This observation implies that increasing voltages initially increase resistance due to higher polarisation or slower reaction kinetics. When the voltage surpasses 1.0 V, the impedance starts decreasing, possibly due to enhanced mass transport, thereby decreasing overall impedance.

Cyclic voltammetry (CV) was conducted to determine whether biomass could be directly oxidised on the graphite electrode. The resulting voltammograms (I vs V) were analysed to identify oxidation and reduction peaks, which indicate electrochemical reactions occurring at the electrode surface. Fig. S4 (c) displays the cyclic voltammetry curves of pure PMo_{12}, PMo_{12}-banana peel and PMo_{12}-cucumber peel solutions within the potential range of −1.2 V–1.2 V vs Ag/AgCl at a scan rate of 50 mV/s (three-electrode system was employed for conducting CV such as graphite electrode (working electrode), Ag/AgCl (reference electrode) and platinum mesh (counter electrode)). Cyclic voltammetry analysis of PMo_{12}-banana peel and PMo_{12}-cucumber peel solutions revealed that no additional peaks emerged, and the redox peaks were consistent with those observed in pure PMo_{12}, which indicates that biomass cannot be directly degraded on a graphite electrode. The reduced PMo_{12} released the electrons to the graphite electrode and reoxidised to its original form [17].

3.6. Hydrogen generation rate via biomass electrolysis

An experimental study of the PMo_{12}-banana and PMo_{12}-cucumber biomass electrolysis system was performed for up to 20 h to estimate the total amount of hydrogen produced by 0.5 g of biomass and understand the hydrogen generation rate. The chronoamperometry technique (an electrochemical technique where the current is measured over time while the potential of the working electrode is held constant) was used to assess the hydrogen generation via an h-type PEM electrolysis cell at a constant voltage of 1.20 V. Fig. 4(a and b) illustrates the electrolytic current and hydrogen production rate for both biowastes. The chronoamperometry test revealed that the rate of hydrogen formation was highest in the first hour of electrolysis, reaching 6.8 mL with banana peel and 5.7 mL with cucumber peel. Over the 20 h electrolysis period, hydrogen productivity gradually decreased, resulting in total yields of 49.2 mL and 39.9 mL for banana and cucumber peels, respectively. A limited amount of H_2 was observed during the banana peel electrolysis experiment in the range of 40,000–72,000 s, while in the case of the cucumber peel, a limited H_2 yield was obtained during 30,000–72,000 s. This gradual decrease in H_2 yield with electrolytic current is attributed to the batch-processing nature of the system because continuous feeding was not provided [20].

The reoxidation of PMo_{12} was also confirmed by the colour transformation throughout the chronoamperometry, as described in literature studies [17,46]. Initially, with the introduction of banana and cucumber peels into the PMo_{12} solution, the colour of the solution turned green (Fig. S5). The green colour of the solution shifted to dark blue during the pre-treatment process, indicating that the biomass and PMo_{12} undergo redox reaction (i.e. $PMo_{12\ reduced}$). During the electrolysis process, the solution colour reverted to green, which demonstrates the reoxidation of the reduced PMo_{12} [42].

The reaction mechanism of the PMo_{12}-biomass electrolysis system can be seen in Eqs. (1)–(3).

Pre-treatment step:

$$Biomass + PMo_{12} + water \rightarrow H - PMo_{12(reduced)} + CO_2 + oxidised\ Products \quad (1)$$

Electrolysis step:

Anode:

$$H - PMo_{12(reduced)} \rightarrow PMo_{12(oxidised)} + H^+ + e^- \quad (2)$$

Cathode:

$$H^+ + e^- \rightarrow \frac{1}{2}H_2 \quad (3)$$

To demonstrate the degradation of biomasses like banana and cucumber peels, pure and PMo_{12}-oxidised solid residues were analysed by FTIR, as shown in Fig. 5(a and b). The FTIR spectra of banana and cucumber peels revealed that the absorption bands in the region 3344.85 cm^{-1} and 3293.57 cm^{-1} are attributed to the stretching of strong O-H groups. After pre-treatment with PMo_{12}, the peak strength reduced, and a slight shift in the peaks was observed, suggesting the disruption of hydrogen bonds in the banana and cucumber peels. Meanwhile, peaks originating at 2916.82 cm^{-1} (banana peel) and 2922.64 cm^{-1} (cucumber peel) are associated with the stretching vibrations of the C-H stretching of methyl and methylene groups. The absorption bands in the region of 1800 cm^{-1}-800 cm^{-1} represent the characteristic peaks of significant components of biomasses such as lignin, hemicellulose and cellulose [67]. The absorption peak at 1736.14 cm^{-1} in the banana peel FTIR spectrum represents the carboxylic acid and stretching vibration of C=O in hemicellulose. In the case of cucumber, the peaks originated at 1731.60 cm^{-1} and 1238 cm^{-1} shows the characteristic absorption peaks of hemicellulose [68]. These absorption bands were reduced after oxidation with PMo_{12}, indicating the degradation of hemicellulose a key

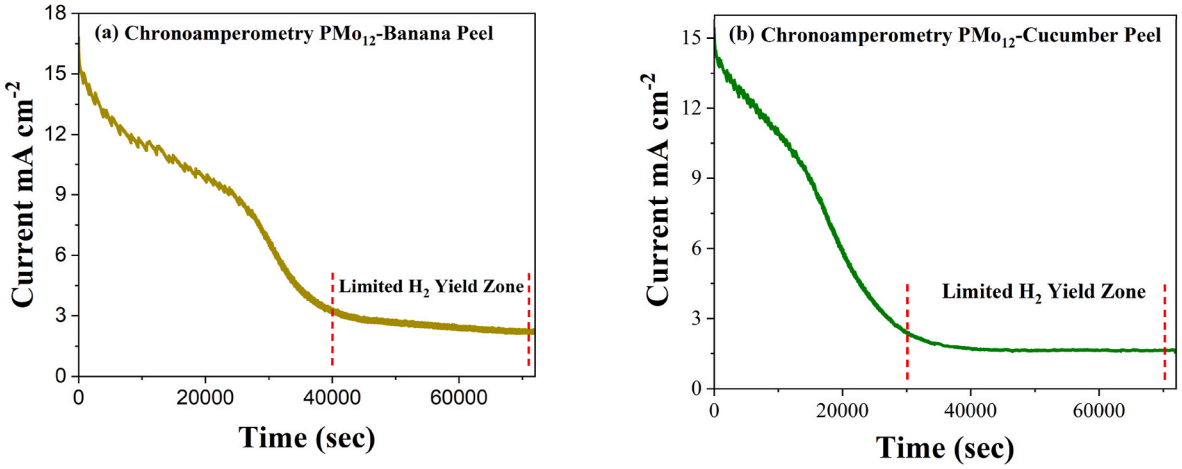

Fig. 4. Chronoamperometry analysis of (a) PMo_{12}-banana peel and (b) PMo_{12}-cucumber peel electrolysis system for H_2 production.

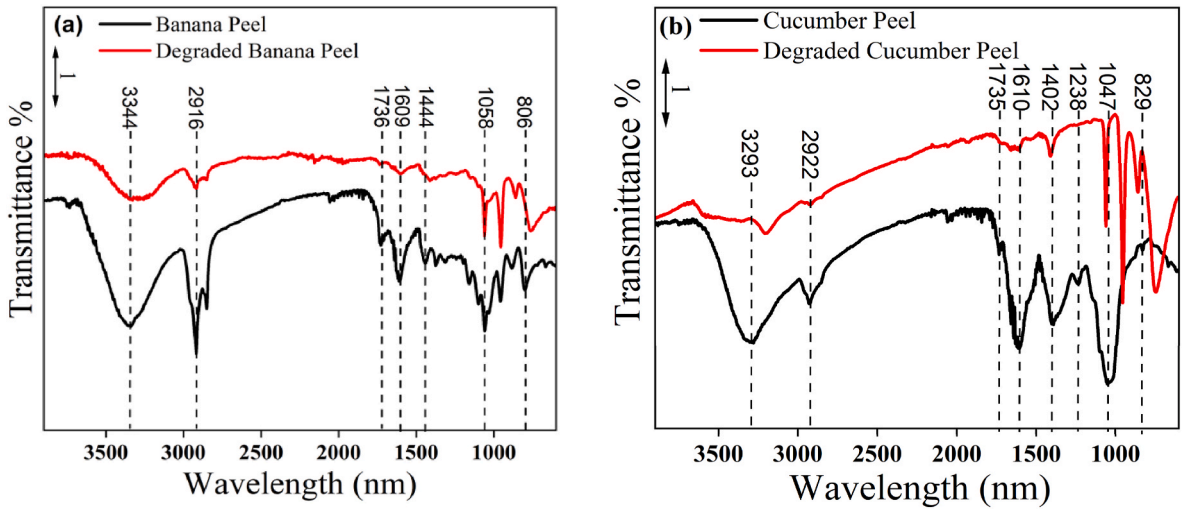

Fig. 5. FTIR analysis of before and after oxidation with PMo_{12} (a) banana peel and (b) cucumber peel.

component of banana and cucumber peels. The absorption peaks at 1609.03 cm^{-1} and 1444.57 cm^{-1} in the FTIR spectra of banana peel correspond to the lignin characteristics peaks. In the case of cucumber peel, lignin peaks originated at 1610.46 cm^{-1} and 1402.05 cm^{-1} [69,70]. The decrease in these peaks' intensity after being oxidised with PMo_{12} indicates that the lignin content in the peels has been significantly converted. The absorption band at 1158.12 cm^{-1} (banana peel) and 1047.15 cm^{-1} (cucumber peel) corresponds to the characteristic peaks of cellulose [71,72]. The peaks at 806.11 cm^{-1} and 829.24 cm^{-1} represent the crystalline structure of cellulose in banana and cucumber peels [72]. Therefore, no observable changes occurred in the peaks' intensity of cellulose in banana and cucumber peels FTIR spectra after pre-treatment. So, the cellulose remains largely unaffected after oxidation with PMo_{12}, indicating that the cellulose remains the predominant component in the biomass residues. In contrast, hemicellulose and lignin peaks show a decreasing trend, demonstrating degradation.

UV–visible analysis was conducted to investigate the reduction of PMo_{12} during the degradation process between PMo_{12} and biomass, where biomass becomes oxidised by the reduction of PMo_{12} (Fig. 6(a and b)). The reduction degree of PMo_{12} is described as the average number of electrons transferred from the biomass to 1 mol of PMo_{12} anion [73]. Evolution 220 UV–visible spectrophotometer was employed to obtain the UV–visible spectrum of PMo_{12}-banana and PMo_{12}-cucumber peel solutions. The reduction level of PMo_{12} can be determined by measuring its absorbance at 740 nm due to its linear correlation with the absorbance of reduced PMo_{12} at this wavelength. For absorbance determination at 700 nm, various samples (i.e. 1 mL by syringe) were collected during the degradation process of both banana and cucumber peels and then diluted to 1 mmol/L of the total concentration of PMo_{12} employed for the UV–visible spectrometry [17,42].

Fig. 6 (a) demonstrates that the reduction of PMo_{12} sharply increased after 1 h, showing that the banana peel can be degraded quickly. However, this PMo_{12} reduction phenomenon slowly increased during the third hour, possibly due to reaction kinetic limitations such as slow electron transfer rate or substrate diffusion barriers that can slow the movement of particles or molecules from one area to another [46,74]. After the third hour, the reaction accelerates again, and more PMo_{12} reduction is seen in the UV spectra. However, the UV peak did not significantly increase during the fifth hour, suggesting that the reaction between PMo_{12} and the banana peel is nearing completion. Similarly, for the cucumber-PMo_{12} solution, the absorbance curves gradually increased with reaction time, but their absorbance rate was lowered compared to the PMo_{12}-banana peel solution, as shown in Fig. 6 (b). The lower absorbance of the PMo_{12}-cucumber solution is derived from the higher percentage of cellulose in its structural composition, as demonstrated by the elemental analysis (Table S1). This indicates that the higher the absorbance, the higher the concentration of reduced PMo_{12} and the more biomass degraded during the degradation reaction [54].

Further, the conversion efficiency of biomass material was also estimated based on the weight ratio of the hydrogen produced and the

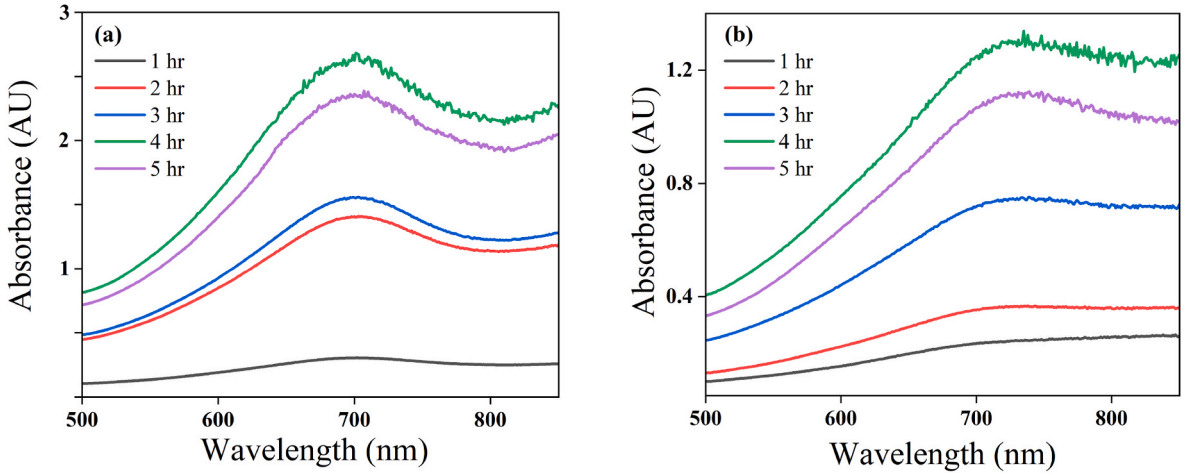

Fig. 6. UV visible spectrum of (a) PMo_{12}-banana peel solution and (b) PMo_{12}-cucumber peel solution.

one contained in banana and cucumber peels, as presented in Table S4. The conversion efficiency of H-content for banana and cucumber peels was 17 % and 10 %, respectively. Values obtained are in line with values recorded by other biomass-to-hydrogen conversion processes. For example, gasification of tea waste at temperatures ranging from 450 to 850 °C through an air gasification process achieved a hydrogen content conversion efficiency of 13.3 % [75]. Similarly, the hydrogen conversion efficiency of lignin into hydrogen via the supercritical water gasification method was 23.82 % [76].

The fact that banana peel produces more hydrogen than cucumber peel, although its hydrogen contact is lower (4.9 wt % towards 6.98 wt %), shows the role played by the structural composition of biomass. Cucumber peel contains a high percentage of cellulose (17 wt %) and low percentages of lignin (5.05 wt %) and hemicellulose (5.6 wt %) in comparison to banana peel, which has lower cellulose content (9.6 wt %), and higher hemicellulose (9.4 wt %) & lignin content (12 wt %). As discussed above, cellulose degradation is more difficult than hemicellulose and lignin.

Regarding energy efficiency, the estimated power-to-H_2 yield ratios for banana and cucumber peels were 35.35 kWh/kg and 42.17 kWh/kg, respectively, based on the 1-hr hydrogen yield and current density. These findings align closely with recent studies, where the calculated power-to-H_2 yield ratios for corn straw [46] and lignin [20] were 30.58 kWh/kg and 30.35 kWh/kg. While water electrolysis requires around 47–63 kWh of energy to produce 1 kg of hydrogen [8]. The comparison indicates that biomass electrolysis can be 20–45 % more energy-efficient than conventional water electrolysis if we only account for the electricity required. Therefore, biomass electrolysis has the potential to produce clean hydrogen fuel at a lower operating cost.

4. Conclusion

The present study used lignocellulosic biomass components and food waste as feedstocks to investigate hydrogen generation through polyoxometalate-catalysed electrolysis to understand the correlation between biomass components and hydrogen production and the influence of the main operating parameters. The study demonstrated the feasibility of producing hydrogen from biomass components and biowaste at ambient and relatively low temperatures (80 °C). The study showed that different biomass components have different potentials for hydrogen production, with the highest hydrogen production recorded for glucose and the minimum for cellulose. The superior performance of glucose is attributed to its ease of degradation by PMo_{12}. Additionally, it was found that banana peel showed higher hydrogen production (49.2 mL versus 39.6 mL). However, the hydrogen content of banana peel was lower than that of cucumber peel (4.9 wt % versus 6.98 wt %). This higher hydrogen production is due to the higher hemicellulose and lignin and lower cellulose content in the banana peel. It was also shown that temperature and pre-treatment duration can boost hydrogen production; however, after a certain point, the production did not increase as predicted, possibly because of mass transfer limitations. To improve the process conversion efficiency, which is currently less than 20 %, further research must concentrate on three areas: optimising biomass degradation, effectively reusing catalysts and extracting additional value from the electrolysis residue.

CRediT authorship contribution statement

Muhammad Umer: Writing – original draft, Methodology, Investigation. **Caterina Brandoni:** Writing – review & editing, Supervision. **Svetlana Tretsiakova:** Resources, Conceptualization. **Neil Hewitt:** Supervision, Conceptualization. **Patrick Dunlop:** Writing – review & editing, Conceptualization. **M.D. Mokim:** Data curation. **Kai Zhang:** Conceptualization. **Ye Huang:** Writing – review & editing, Supervision.

Declaration of competing interest

The authors declare that they have no known competing financial interests or personal relationships that could have appeared to influence the work reported in this paper.

Data availability

Data will be made available on request.

Acknowledgement

This study was funded by the Department for the Economy (DfE), Northern Ireland, United Kingdom. Muhammad Umer is a Doctoral Scholar at the Faculty of Computing, Engineering and the Built Environment at Ulster University, Belfast (Northern Ireland, United Kingdom). This research work was also carried out as part of the Royal Society and National Natural Science Foundation of China (IEC\NSFC \201070).

Appendix A. Supplementary data

Supplementary data to this article can be found online at https://doi.org/10.1016/j.rineng.2024.102803.

References

[1] M.U. Azam, W. Afzal, A. Fernandes, I. Graça, Insights into the development of greener mild zeolite dealumination routes applied to the hydrocracking of waste plastics (2024) 119873.
[2] M.U. Azam, W. Afzal, I.J.C. Graça, Advancing Plastic Recycling: A Review on the Synthesis and Applications of Hierarchical Zeolites in Waste Plastic Hydrocracking (2024).
[3] H. Sun, L. Li, Y. Chen, H. Kim, X. Xu, D. Guan, et al., Boosting Ethanol Oxidation by NiOOH-CuO Nano-Heterostructure for Energy-Saving Hydrogen Production and Biomass Upgrading (2023) 122388.
[4] V. Deivayanai, P. Yaashikaa, P.S. Kumar, G.J.B.T. Rangasamy, A Comprehensive Review on the Biological Conversion of Lignocellulosic Biomass into Hydrogen: Pre-treatment Strategy, Technology Advances and Perspectives, vol. 365, 2022 128166.
[5] E. Chalhoub, Belovich JmjriE, Mathematical modeling of fermentation from glucose, xylose, and food waste of clostridia sp, Strain BOH3 for the Production of ABE Solvents and Hydrogen (2024) 102366.
[6] C.L. Yiin, A.T. Quitain, S. Yusup, Y. Uemura, M. Sasaki, Kida Tjbt, Sustainable green pre-treatment approach to biomass-to-energy conversion using natural hydro-low-transition-temperature mixtures 261 (2018) 361–369.
[7] L. Cao, K. Iris, X. Xiong, D.C. Tsang, S. Zhang, J.H. Clark, et al., Biorenewable Hydrogen Production through Biomass Gasification: A Review and Future Prospects, vol. 186, 2020 109547.
[8] MJRiE. El-Shafie, Hydrogen production by water electrolysis technologies: Review (2023) 101426.
[9] Q. Wang, X. Zhang, D. Cui, J. Bai, Z. Wang, F. Xu, et al., Advances in Supercritical Water Gasification of Lignocellulosic Biomass for Hydrogen Production, vol. 170, 2023 105934.
[10] R. Morya, T. Raj, Y. Lee, A.K. Pandey, D. Kumar, R.R. Singhania, et al., Recent Updates in Biohydrogen Production Strategies and Life–Cycle Assessment for Sustainable Future, vol. 366, 2022 128159.
[11] H. Kachroo, V.K. Verma, T.R.K.C. Doddapaneni, P. Kaushal, R.J.B.T. Jain, Organometallic-component analysis of lignocellulosic biomass: A thermochemical-perspective-based study on rice and bamboo waste (2024) 130835.
[12] A. Saravanakumar, P. Vijayakumar, A.T. Hoang, E.E. Kwon, W. Chen, Hjbt, Thermochemical Conversion of Large-Size Woody Biomass for Carbon Neutrality: Principles, Applications, and Issues, vol. 370, 2023 128562.
[13] G. Kong, Q. Liu, G. Ji, H. Jia, T. Cao, X. Zhang, et al., Improving Hydrogen-Rich Gas Production from Biomass Catalytic Steam Gasification over Metal-Doping Porous Biochar, vol. 387, 2023 129662.
[14] Y.S. Yong, Rasid RajijoHE, Process Simulation of Hydrogen Production through Biomass Gasification: Introduction of Torrefaction Pre-treatment, vol. 47, 2022, pp. 42040–42050.
[15] S.K. Dash, S. Chakraborty, D.J.E. Elangovan, A Brief Review of Hydrogen Production Methods and Their Challenges, vol. 16, 2023, p. 1141.
[16] S. Shanmugam, T. Mathimani, K. Rajendran, M. Sekar, E.R. Rene, N.T.L. Chi, et al., Perspective on the Strategies and Challenges in Hydrogen Production from Food and Food Processing Wastes, vol. 338, 2023 127376.
[17] W. Liu, Y. Cui, X. Du, Z. Zhang, Z. Chao, Y.J.E. Deng, et al., High Efficiency Hydrogen Evolution from Native Biomass Electrolysis, vol. 9, 2016, pp. 467–472.
[18] X. Lu, S. Xie, H. Yang, Y. Tong, H.J.C.S.R. Ji, Photo-electrochemical Hydrogen Production from Biomass Derivatives and Water, vol. 43, 2014, pp. 7581–7593.

[19] W. Liu, C. Liu, P. Gogoi, Y.J.E. Deng, Overview of Biomass Conversion to Electricity and Hydrogen and Recent Developments in Low-Temperature Electrochemical Approaches, vol. 6, 2020, pp. 1351–1363.
[20] M. Li, T. Wang, X. Chen, X. Ma, Conversion study from lignocellulosic biomass and electric energy to H2 and chemicals (2022).
[21] C. Dolle, N. Neha, C. Coutanceau, Electrochemical Hydrogen Production from Biomass, vol. 31, 2022 100841.
[22] M. Umer, C. Brandoni, M. Jaffar, N.J. Hewitt, P. Dunlop, K. Zhang, et al., An Experimental Investigation of Hydrogen Production through Biomass Electrolysis, vol. 12, 2024, p. 112.
[23] H. Luo, J. Barrio, N. Sunny, A. Li, L. Steier, N. Shah, et al., Progress and Perspectives in Photo-and Electrochemical-oxidation of Biomass for Sustainable Chemicals and Hydrogen Production, vol. 11, 2021 2101180.
[24] M. Rezayeenik, M. Mousavi-Kamazani, S.J.A.P.A. Zinatloo-Ajabshir, CeVO4/rGO Nanocomposite: Facile Hydrothermal Synthesis, Characterisation, and Electrochemical Hydrogen Storage, vol. 129, 2023, p. 47.
[25] A. Zonarsaghar, M. Mousavi-Kamazani, S. Zinatloo-Ajabshir, Sonochemical Synthesis of CeVO4 Nanoparticles for Electrochemical Hydrogen Storage, vol. 47, 2022, pp. 5403–5417.
[26] M.H. Esfahani, S. Zinatloo-Ajabshir, H. Naji, C.A. Marjerrison, J.E. Greedan, M.J.C. I. Behzad, Structural characterisation, phase analysis and electrochemical hydrogen storage studies on new pyrochlore SmRETi2O7 (RE= Dy, Ho, and Yb) microstructures 49 (2023) 253–263.
[27] S. Zinatloo-Ajabshir, Z. Salehi, O. Amiri, MJIjohe Salavati-Niasari, Green Synthesis, Characterisation and Investigation of the Electrochemical Hydrogen Storage Properties of Dy2Ce2O7 Nanostructures with Fig Extract, vol. 44, 2019, pp. 20110–20120.
[28] A.K. Islam, P.S. Dunlop, G. Bhattacharya, M. Mokim, N.J. Hewitt, Y. Huang, et al., Comparative Performance of Sustainable Anode Materials in Microbial Fuel Cells (MFCs) for Electricity Generation from Wastewater, vol. 20, 2023 101385.
[29] H.-O. Lee, J. Yesuraj, K.J.A.E. Kim, Parametric study to optimise proton exchange membrane electrolyser cells 314 (2022) 118928.
[30] P.A. Selembo, J.M. Perez, W.A. Lloyd, BEJIjohe Logan, High Hydrogen Production from Glycerol or Glucose by Electrohydrogenesis Using Microbial Electrolysis Cells, vol. 34, 2009, pp. 5373–5381.
[31] M.T. Anwar, X. Yan, S. Shen, N. Husnain, F. Zhu, L. Luo, et al., Enhanced Durability of Pt Electrocatalyst with Tantalum Doped Titania as Catalyst Support, vol. 42, 2017, pp. 30750–30759.
[32] M. Rashid, M.K. Al Mesfer, H. Naseem, M. Danish, A. Technology, Hydrogen production by water electrolysis: a review of alkaline water electrolysis. PEM Water Electrolysis and High Temperature Water Electrolysis, 2015.
[33] A. Jamil, S. Rafiq, T. Iqbal, H.A.A. Khan, H.M. Khan, B. Azeem, et al., Current status and future perspectives of proton exchange membranes for hydrogen fuel cells (2022) 135204.
[34] A. Salari, A. Hakkaki-Fard, Jalalidil AjijoHE, Hydrogen production performance of a photovoltaic thermal system coupled with a proton exchange membrane electrolysis cell 47 (2022) 4472–4488.
[35] Y. Wang, M. Zhao, T. Wang, M. Li, X. Lu, Li BjijoHE, Study on Hydrogen Generation and Cornstalk Degradation by Redox Coupling of Non-noble Metal Fe3+/Fe2+, vol. 46, 2021, pp. 27409–27421.
[36] A. Caravaca, W.E. Garcia-Lorefice, S. Gil, A. de Lucas-Consuegra, P.J.E.C. Vernoux, Towards a Sustainable Technology for H2 Production: Direct Lignin Electrolysis in a Continuous-Flow Polymer Electrolyte Membrane Reactor, vol. 100, 2019, pp. 43–47.
[37] T. Hibino, K. Kobayashi, M. Ito, M. Nagao, M. Fukui, S. Teranishi, Direct Electrolysis of Waste Newspaper for Sustainable Hydrogen Production: an Oxygen-Functionalised Porous Carbon Anode, vol. 231, 2018, pp. 191–199.
[38] M. Ito, T. Hori, S. Teranishi, M. Nagao, TJSr Hibino, Intermediate-temperature Electrolysis of Energy Grass Miscanthus Sinensis for Sustainable Hydrogen Production, vol. 8, 2018, pp. 1–9.
[39] Z.I. Lai, L.Q. Lee, H.J.M. Li, Electroreforming of Biomass for Value-Added Products, vol. 12, 2021, p. 1405.
[40] L. Wu, J. Liang, Polyoxometalates and their complexes toward biological application (2017) 311–354.
[41] H. Guo, Y. Wang, L. Tian, W. Wei, T. Zhu, Y.J.B.T. Liu, Unveiling the Mechanisms of a Novel Polyoxometalates (POMs)-Based Pre-treatment Technology for Enhancing Methane Production from Waste Activated Sludge, vol. 342, 2021 125934.
[42] M. Li, T. Wang, M. Zhao, Y. Wang, Research on Hydrogen Production and Degradation of Corn Straw by Circular Electrolysis with Polyoxometalate (POM) Catalyst, vol. 47, 2022, pp. 15357–15369.
[43] R. Price, L. MacDonald, N. Gillies, A. Day, E. Brightman, J.J.F.D. Li, Utilisation and Valorisation of Distillery Whisky Waste Streams via Biomass Electrolysis: Electrosynthesis of Hydrogen (2023).
[44] W. Liu, W. Mu, M. Liu, X. Zhang, H. Cai, YJNc Deng, Solar-induced Direct Biomass-To-Electricity Hybrid Fuel Cell Using Polyoxometalates as Photocatalyst and Charge Carrier, vol. 5, 2014, p. 3208.
[45] H. Oh, Y. Choi, C. Shin, T.V.T. Nguyen, Y. Han, H. Kim, et al., Phosphomolybdic Acid as a Catalyst for Oxidative Valorisation of Biomass and its Application as an Alternative Electron Source, vol. 10, 2020, pp. 2060–2068.
[46] M. Li, T. Wang, M. Zhao, Y. Wang, Research on hydrogen production and degradation of corn straw by circular electrolysis with polyoxometalate (POM) catalyst (2021).
[47] M. Ito, T. Hori, S. Teranishi, M. Nagao, T.J.S.R. Hibino, Intermediate-temperature Electrolysis of Energy Grass Miscanthus Sinensis for Sustainable Hydrogen Production, vol. 8, 2018 16186.
[48] M. Wu, J. Di, L. Gong, Y.-C. He, C. Ma, Y.J.C.E.J. Deng, Enhanced Adipic Acid Production from Sugarcane Bagasse by a Rapid Room Temperature Pre-treatment, vol. 452, 2023 139320.
[49] R.K. Rathour, M. Devi, P. Dahiya, N. Sharma, N. Kaushik, D. Kumari, et al., Recent Trends, Opportunities and Challenges in Sustainable Management of Rice Straw Waste Biomass for Green Biorefinery, vol. 16, 2023, p. 1429.
[50] B. Erdei, Z. Barta, B. Sipos, K. Réczey, M. Galbe, GJBfB. Zacchi, Ethanol Production from Mixtures of Wheat Straw and Wheat Meal, vol. 3, 2010, pp. 1–9.
[51] W. Liu, W. Mu, Y. Deng, High-performance Liquid-catalyst Fuel Cell for Direct Biomass-into-electricity Conversion, vol. 53, 2014, pp. 13558–13562.
[52] D.B. Pal, A. Singh, A. Bhatnagar, A Review on Biomass Based Hydrogen Production Technologies, vol. 47, 2022, pp. 1461–1480.
[53] M. Li, T. Wang, X. Chen, X. Ma, Conversion Study from Lignocellulosic Biomass and Electric Energy to H2 and Chemicals, vol. 48, 2023, pp. 21004–21017.
[54] W. Xu, B. Zhou, Q. Wang, G. Xu, N. Li, W. Liu, et al., Energy-efficient Electrochemical Hydrogen Production Combined with Biomass Oxidation Using Polyoxometalate and Metal Salts, vol. 15, 2023 e202300522.
[55] W. Liu, Y. Gong, W. Wu, W. Yang, C. Liu, Y. Deng, et al., Efficient Biomass Fuel Cell Powered by Sugar with Photo-and Thermal-Catalysis by Solar Irradiation, vol. 11, 2018, pp. 2229–2238.
[56] X. Du, W. Liu, Z. Zhang, A. Mulyadi, A. Brittain, J. Gong, et al., Low-energy Catalytic Electrolysis for Simultaneous Hydrogen Evolution and Lignin Depolymerisation, vol. 10, 2017, pp. 847–854.
[57] W. Zhao, B. Simmons, S. Singh, A. Ragauskas, G.J.G.C. Cheng, From Lignin Association to Nano-/micro-Particle Preparation: Extracting Higher Value of Lignin, vol. 18, 2016, pp. 5693–5700.
[58] E.E. Oliveira, A.E. Silva, T.N. Júnior, M.C.S. Gomes, L.M. Aguiar, H.R. Marcelino, et al., Xylan from Corn Cobs, a Promising Polymer for Drug Delivery: Production and Characterisation, vol. 101, 2010, pp. 5402–5406.
[59] S.B. Aziz, B. Marif R, M. Brza, M. Hamsan, M.J.P. Kadir, Employing of Trukhan Model to Estimate Ion Transport Parameters in PVA Based Solid Polymer Electrolyte, vol. 11, 2019, p. 1694.
[60] S. Xiao, L. Yu, L. Wu, L. Liu, X. Qiu, J.J.E.A. Xi, Broad Temperature Adaptability of Vanadium Redox Flow Battery—Part 1: Electrolyte Research, vol. 187, 2016, pp. 525–534.
[61] Demirel SjijoES, Temperature Dependent Polarisation Effect and Capacitive Performance Enhancement of PVA-Borax Gel Electrolyte, vol. 15, 2020, pp. 2439–2448.
[62] J. Gao, L. Chen, J. Zhang, ZJBt Yan, Improved Enzymatic Hydrolysis of Lignocellulosic Biomass through Pre-treatment with Plasma Electrolysis, vol. 171, 2014, pp. 469–471.
[63] Y. Zhao, X. Jia, Q. Wang, Y. Wu, Z. Jia, X. Zhou, et al., PMo12 as a Redox Mediator for Bio-Reduction of Cr (VI): Promotor or Inhibitor?, vol. 859, 2023 159896.
[64] Z. Lukács, T.J.E.A. Kristóf, A Generalised Model of the Equivalent Circuits in the Electrochemical Impedance Spectroscopy, vol. 363, 2020 137199.
[65] P. Leuaa, D. Priyadarshani, D. Choudhury, R. Maurya, Neergat Mjra, Resolving Charge-Transfer and Mass-Transfer Processes of VO 2+/VO 2+ Redox Species across the Electrode/electrolyte Interface Using Electrochemical Impedance Spectroscopy for Vanadium Redox Flow Battery, vol. 10, 2020, pp. 30887–30895.
[66] T. Hibino, K. Kobayashi, M. Ito, Q. Ma, M. Nagao, M. Fukui, et al., Efficient Hydrogen Production by Direct Electrolysis of Waste Biomass at Intermediate Temperatures, vol. 6, 2018, pp. 9360–9368.
[67] Z. Jiang, J. Yi, J. Li, T. He, C.J.C. Hu, Promoting Effect of Sodium Chloride on the Solubilisation and Depolymerisation of Cellulose from Raw Biomass Materials in Water, vol. 8, 2015, pp. 1901–1907.
[68] X.-M. Zhang, L.-Y. Meng, F. Xu, R.-C.J.I.C. Sun, Products. Pre-treatment of partially delignified hybrid poplar for biofuels production: Characterisation of organosolv hemicelluloses 33 (2011) 310–316.
[69] S.S. Tan, D.R. MacFarlane, J. Upfal, L.A. Edye, W.O. Doherty, A.F. Patti, et al., Extraction of Lignin from Lignocellulose at Atmospheric Pressure Using Alkylbenzenesulfonate Ionic Liquid, vol. 11, 2009, pp. 339–345.
[70] A. Tejado, C. Pena, J. Labidi, J. Echeverria, Mondragon Ijbt, Physico-chemical characterisation of lignins from different sources for use in phenol–formaldehyde resin synthesis 98 (2007) 1655–1663.
[71] A.J. Kunov-Kruse, A. Riisager, S. Saravanamurugan, R.W. Berg, S.B. Kristensen, Fehrmann Rjgc, Revisiting the Brønsted Acid Catalysed Hydrolysis Kinetics of Polymeric Carbohydrates in Ionic Liquids by in Situ ATR-FTIR Spectroscopy, vol. 15, 2013, pp. 2843–2848.
[72] J. Long, X. Li, B. Guo, F. Wang, Y. Yu, LJGc Wang, Simultaneous Delignification and Selective Catalytic Transformation of Agricultural Lignocellulose in Cooperative Ionic Liquid Pairs, vol. 14, 2012, pp. 1935–1941.
[73] W. Liu, W. Mu, Y.J.A.C. Deng, High-performance Liquid-catalyst Fuel Cell for Direct Biomass-into-electricity Conversion, vol. 126, 2014, pp. 13776–13780.
[74] B. Gamisch, L. Huber, M. Gaderer, B.J.E. Dawoud, On the Kinetic Mechanisms of the Reduction and Oxidation Reactions of Iron Oxide/iron Pellets for a Hydrogen Storage Process, vol. 15, 2022, p. 8322.
[75] N. Ayas, TJijohe Esen, Hydrogen Production from Tea Waste, vol. 41, 2016, pp. 8067–8072.
[76] C. Cao, L. Yu, Y. Xie, W. Wei, H. Jin, Hydrogen Production by Supercritical Water Gasification of Lignin over CuO–ZnO Catalyst Synthesised with Different Methods, vol. 47, 2022, pp. 8716–8728.